



UNIVERSITY OF LEEDS

This is a repository copy of *Cascading Failures in Interconnected Power-to-Water Networks*.

White Rose Research Online URL for this paper:
<http://eprints.whiterose.ac.uk/165735/>

Version: Accepted Version

Article:

Pournaras, E, Taormina, R, Thapa, M et al. (3 more authors) (2020) Cascading Failures in Interconnected Power-to-Water Networks. *ACM SIGMETRICS Performance Evaluation Review*, 47 (4). pp. 16-20. ISSN 0163-5999

<https://doi.org/10.1145/3397776.3397781>

Copyright is held by author/owner(s). This is an author produced version of a journal article published in *ACM SIGMETRICS Performance Evaluation Review*. Uploaded in accordance with the publisher's self-archiving policy.

Reuse

Items deposited in White Rose Research Online are protected by copyright, with all rights reserved unless indicated otherwise. They may be downloaded and/or printed for private study, or other acts as permitted by national copyright laws. The publisher or other rights holders may allow further reproduction and re-use of the full text version. This is indicated by the licence information on the White Rose Research Online record for the item.

Takedown

If you consider content in White Rose Research Online to be in breach of UK law, please notify us by emailing eprints@whiterose.ac.uk including the URL of the record and the reason for the withdrawal request.



eprints@whiterose.ac.uk
<https://eprints.whiterose.ac.uk/>

Cascading Failures in Interconnected Power-to-Water Networks

Evangelos Pournaras
ETH Zurich
epournaras@ethz.ch

Riccardo Taormina
TU Delft
r.taormina@tudelft.nl

Manish Thapa
ETH Zurich
manish.thapa@phys.chem.ethz.ch

Stefano Galelli
SUTD
stefano_galelli@sutd.edu.sg

Venkata Palleti
SUTD
venkata_palleti@sutd.edu.sg

Robert Kooij
TU Delft
r.e.kooij@tudelft.nl

ABSTRACT

The manageability and resilience of critical infrastructures, such as power and water networks, is challenged by their increasing interdependence and interconnectivity. Power networks often experience cascading failures, i.e. blackouts, that have unprecedented economic and social impact. Although knowledge exists about how to control such complex non-linear phenomena within a single power network, little is known about how such failures can spread and coevolve in the water network when failing power components energize the water distribution infrastructure, i.e. pumps and valves. This paper studies such a scenario and specifically the impact of power cascading failures on shortages of water supply. A realistic exemplar of an interconnected power-to-water network is experimentally evaluated using a modular simulation approach. Power and water flow dynamics are simulated separately by taking into account different maximum power lines capacities and water demand requirements. Results showcase the strong dependency of urban water supply systems on the reliability of power networks, with severe shortages of water supply being caused by failures originating in distant power lines, especially for heavily loaded power networks.

1. INTRODUCTION

Coupling critical infrastructures together, such as power and water networks, puts at risk their resilience [7]. Power networks can be highly vulnerable to components failures that can cause cascading failures and influence other components that energize pumps and valves of the water network. The function of the latter influences the water supply distribution in the whole network. These interdependencies challenge the manageability of such coupled critical infrastructures as dynamics over interconnected networks are fundamentally different and more complex than the ones of isolated networks [12, 1]. Spreading and coevolving failures from one network to the other can cause unforeseen economic damages and social unrest of an unprecedented impact [2, 7].

Previous studies have shown the impact of failures of power networks interconnected with Internet [6] and gas distribution networks [21]. [10] studied the effects of limited electrical

power availability on water distribution for power-to-water interconnected networks. The authors considered only static power grid failure conditions, and focused on devising optimal control strategies of the hydraulic components (pumps and valves) to minimize impacts to customers.

On the other hand, this work explicitly considers power flow dynamics to study the impact of power cascading failures on shortages of water supply. In other words, we are concerned with bi-dimensional cascading effects where a failure in the power grid affects the dependent water network by first propagating to the power nodes (load buses) energizing the hydraulic components. In this way, it is possible to assess whether failures of power lines not directly linked to the load buses may disrupt the operations of the interconnected water network. To investigate this important issue, we resort to a realistic synthetic example, and propose a modular simulation approach where power and water flow dynamics are simulated separately. Multiple experiments are carried out to evaluate the impacts of the cascading failures for different maximum capacities of the power lines and water demand requirements.

This paper is organized as follows: Section 2 introduces the case study studied in this paper—interconnected power-to-water systems.. Section 3 illustrates the experimental settings and evaluation conducted. Finally, Section 4 concludes this paper and outlines future work.

2. CASE STUDY: AN INTERCONNECTED POWER-TO-WATER SYSTEM

We consider a water distribution network that requires interconnection with a power transmission network to energize its hydraulic components, such as pumps and valves. These components are assumed to draw energy from certain load buses in the power network. We study the impact of link failures in the power network on the capability of the water distribution network to satisfy the water demand of consumers. To this end we conduct a $m - 1$ contingency analysis with respect to link failures in the power grid. Such link failures may lead to cascading failures in the power grid. If load buses that energize the water network are affected by the initial power link failure, they will also affect the performance of the water network.

2.1 Cascading failures in power networks

A cascading failure in a power network is typically a re-

sult of power flow redistribution over the network, after an initial link has been tripped, see [19, 11]. The trigger for such an event could be a cyberattack or a system failure. The redistribution is a result of the physical laws that govern power systems. The lines that handle the redistributed power flow also trip if they do not have enough capacity. This can cause further power flow accumulation and spread of the damage. A cascading failure can split the network to several disconnected regions referred to as *islands*. The maximum capacity of a line is imposed by thermal, stability or voltage drop constraints. In our analysis we assume that the maximum capacity C_i of each line i satisfies

$$C_i = \alpha L_i(0), \quad (1)$$

where $L_i(0)$ denotes the initial load of line i , and α is the tolerance parameter. Note that for $\alpha = 1$ the initial system, i.e. before the failures takes place, is fully loaded. This entails that any increase in the load of line i results in a failure.

2.2 Power-to-water interconnection

A water distribution network consists of several hydraulic components—e.g., pipes, tanks, valves or pumps—some of which (e.g., valves, pumps) are actually energized by a power network. In the studied scenario of this paper, the water network is energized by the power network which is experiencing link failures. Each pump and actionable valve is connected to a load bus of the damaged power network from which they draw power. Cascading failures in the power network may cause the deactivation of the load buses and the interruption of power supply to the hydraulic components. This, in turn, may cause localized or system-wide shortages of water supply to customers.

2.3 Performance metric

The demand satisfaction ratio (DSR) evaluates the impact of the power cascading failure on the coupled water network. It is defined as the ratio between the volume of water supplied $w_{s,\tau}$ and demanded $w_{d,\tau}$ in a given time horizon τ :

$$w_\tau = \frac{w_{s,\tau}}{w_{d,\tau}}. \quad (2)$$

DSR varies between 0 and 1, where 0 means that no water is supplied, and 1 that all demanded water is supplied [4].

3. EXPERIMENTAL EVALUATION

This section illustrates the implementation choices, the experimental settings as well as the evaluation results of our power-to-water use case.

3.1 Implementation and experimental settings

For the evaluation we used the IEEE reference power network¹: *case-118*, which contains 118 nodes and 186 links. Different values of the tolerance parameter α are evaluated, with $\alpha \in \{1, 1.2, 1.4, 1.6, 1.8, 2.0\}$. DC power flow analysis, for faster performance and convergence, is performed via

¹Available at <http://www.pserc.cornell.edu/matpower/docs/ref/matpower5.0/menu5.0.html> (last access: December 2018). Case-118 consists of 118 buses, 19 generators, 35 synchronous condensers, 186 lines (including 9 transformers) and 91 loads.

the InterPSS Zhou2007 backend² of SFINA—the *Simulation Framework for Intelligent Network Adaptations* [15, 14]. SFINA is a domain-independent software toolkit for modeling and simulation of the impact of failures and attacks on such interdependent networks. It also allows for prototyping self-management mechanisms³ to make such systems more resilient. SFINA is an open source software implemented in Java under the GPL-2.0 license and is accompanied with a GUI⁴.

The water distribution network studied is the C-Town, depicted in Fig. 1. The C-Town water distribution system is one of the standard benchmark models employed in the field of water distribution system analysis. It is based on a real-world, medium-sized network with 429 pipes and 388 demand nodes [18]. Water storage and distribution in C-Town is guaranteed by 7 tanks (T1 to T7), whose water level controls the operations of one actionable valve (V1) and 11 pumps, spread across 5 pumping stations (S1 to S5). A key element of the network is Pumping station S1, which draws water from the only source and delivers it to Tank T1 as well as several demand nodes. Each pump and the actionable valve are assumed connected to exactly one load bus in *case-118*, from which they draw power.

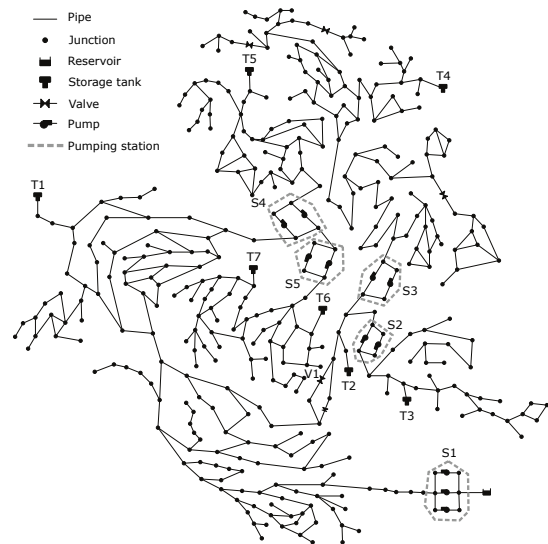


Figure 1: The C-Town water distribution system.

The choices for the water-power interlinks are loosely based on overlaying C-Town on *case-118*. Table 1 shows the interlinks between the C-Town hydraulic components and the load buses of *case-118*. The hydraulic components are switched off (pumps) or disabled (Valve V1) if the corresponding load bus is not energized due to a cascading failure in the

²SFINA currently supports four *domain backends* for network flow calculations: (i) a disaster spread model [3], (ii) MATPOWER [23] and (iii) InterPSS [22] power networks simulation packages, and (iv) MATSim [8] for agent-based transport simulations.

³Implemented *applications* include (i) general-purpose monitoring and measurements of the network topology and flow [19], (ii) simulation of cascading failures in power grids [15] and (iii) coordinated smart transformers for self-repairable smart grids [16].

⁴Available at <https://github.com/SFINA/GUI> (last access: December 2018)

network. In turn, this may affect the operations of C-Town, with localized consequences or network-wide shortages of water supply.

Table 1: Coupling of C-twon and *case-118*.

<i>Hydraulic component</i>	<i>Load bus</i>
Pumping station S1	bus 108
Pumping station S2	bus 118
Pumping station S3	bus 70
Pumping station S4	bus 17
Pumping station S5	bus 20
Actionable valve V1	bus 83

The potential impact of power failures on the water distributed network are simulated with *epanetCPA* [17]; a toolbox built around EPANET, which is the most widely used open-source software for water distribution system analysis. The DSR is computed from *epanetCPA* simulations lasting 2 days, for blackouts lasting 12 hours and starting either at noon or midnight of the first day. Different starting times allow to study the effects of power line failures during periods characterized by the prevalence of high (start=noon) or low water demand (midnight). For a more robust evaluation of the impacts, the DSR is computed for 10 different randomizations of the initial conditions (i.e., initial water levels in the tanks) of C-Town. The same set of random initial conditions are used across all experiments for consistency. In summary, the experiments consist of a total of 22,320 simulations, obtained by crossing the 6x186 power failure scenarios with the 20 scenarios considered in *epanetCPA*.

The use case is evaluated through an $m - 1$ contingency analysis that repeats the following process: a link is removed, the power network (and its coupled water network) undergoes a cascading failure, the DSR metric is computed at every cascade iteration, the network is restored back to its initial state and the whole process repeats for all $m - 1$ link removals. This analysis characterizes probabilistically the overall network reliability, and it is regarded a state of the art evaluation method for power networks [13, 9, 20].

3.2 Interconnected Power-to-Water Network

Table 2 shows the impact of the cascading failures on the 6 load buses that energize C-Town, for the considered values of α . Note that for $\alpha = 1$, on average only 1.1 of the buses remains powered, while always at least one of the load buses is without power. For this α , the removal of 56 out of the 186 links, leave all 6 buses without power. Clearly, the average number of powered buses increases with α .

Table 2: Impact of cascading failures on the 6 buses, shown as the *minimum*, *average* and *maximum* number of buses that still receive power after the cascading failure.

<i>Tolerance parameter α</i>	<i>Min.</i>	<i>Avg.</i>	<i>Max.</i>
1.0	0	1.1	5
1.2	1	3,9	6
1.4	2	5,2	6
1.6	4	5,7	6
1.8	4	5,8	6
2.0	4	5,8	6

Figure 2, which depicts the *case-118* power network, illustrates the relation between failures in the power network and shortage of water supply in C-Town. In particular, the figure shows how the deactivation of a power line in *case-118* influences the DSR of C-Town, where the DSR is averaged across all demand nodes and 10 randomized initial conditions. The thickness and color of each link, are a proxy for the impact of its failure on the DSR. The maps in the first row corresponds to a tolerance parameter $\alpha = 1$ at noon (left) and at midnight (right). The maps in the second row both correspond to a start at noon, with $\alpha = 1.4$ (left) or $\alpha = 1.8$ (right). Shaded bus numbers indicate load buses supplying energy to C-Town hydraulic components. A power line represented with a red thick segment indicates that the damage following an initial failure in that specific line causes severe shortages of water supply across the whole network (low DSR). Intuitively, this happens because the power network disruption disconnects the load buses supplying energy to key hydraulic components, thereby disabling them. On the other hand, thin blue segments indicate that the power line deactivation does not lead to significant cascading failures, that is, the line deactivation does not alter the operations of the interconnected water distribution system (high DSR).

From the maps it is evident that both tolerance parameter α and timing of power line failures have a major impact on DSR. For failures happening at noon, the overall average values of DSR fall to a minimum of 0.872 when the network is at full capacity ($\alpha = 1.0$, Figure 2a). In this scenario, the removal of 56 power lines leave all 6 load buses that energize C-Town, without power. So, all these cases lead to the same low DSR, as depicted by the thick red lines. Note that the removed links do not necessarily need to be close to the buses that energize C-Town, see for instance the low DSR associated with links in the top corners of Figure 2a. This phenomenon progressively disappears when higher values of α are used (Figure 2c and 2d). In these scenarios, the links leading to low DSR values are only the ones causing an outage of bus 108, which energizes the main pumping station S1 (Table 1). For instance, for $\alpha = 1.4$, the removal of link 100-104 leads to a DSR of about 0.85.

Our results further show that events happening at midnight result in similar, but dampened effects on water supply. The reason behind this result stands in the night demand patterns, which are consistently lower than the afternoon ones. Also for the night-time scenarios it is possible to appreciate the importance of links nearby load bus 108, whose deactivation causes substantial reductions of water supply.

Further insights for the events starting at noon are revealed by Figure 3, which illustrates the relation between the percentage of deactivated power lines and the average DSR (for different values of α). For the extreme case of $\alpha = 1.0$, C-Town always experiences a water shortage ($DSR < 1.0$), regardless of which link is initially deactivated. The situation steadily improves as α increases, with only 20% of power line deactivations causing unmet water demands for the highest values of α . This said, it is important to note that, even in the least critical conditions (i.e., $\alpha = 1.8$ or 2.0), there still exists a small fraction of links (around 2%) whose deactivation causes severe water shortages.

4. CONCLUSIONS AND FUTURE WORK

The paper investigates the impact of cascading power fail-

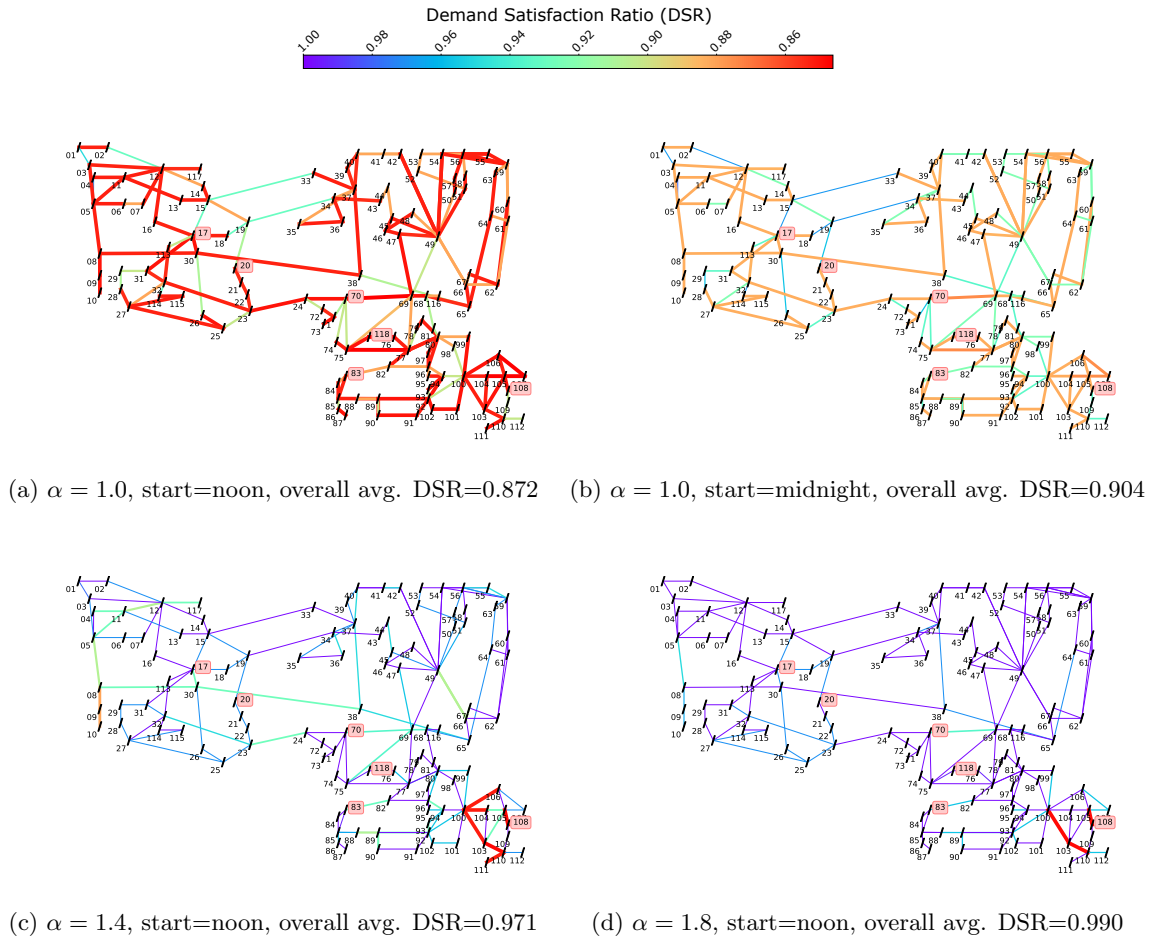


Figure 2: Average DSR due to cascading failures triggered by the deactivation of a power link. The first row corresponds to the case $\alpha = 1$, with power line deactivated at noon (left) and midnight (right). For the second row power line deactivation occurs at noon, with $\alpha = 1.4$ (left) and $\alpha = 1.8$ (right). The reported overall average DSR is the network-wide mean of the average DSR for each demand node. The shaded load buses are those supplying power to the hydraulic components (see Table 1).

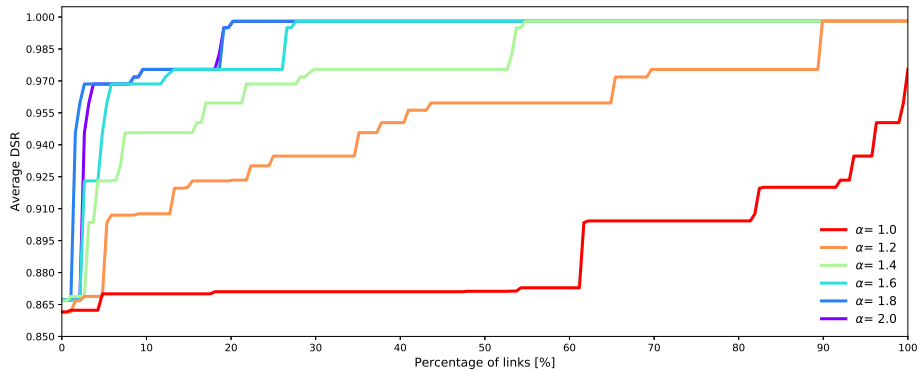


Figure 3: Percentage of deactivated power lines resulting in average DSR below a certain threshold (events starting at noon).

ures on interconnected power-to-water networks. Experiments carried out for a realistic synthetic example show that

cascading effects cause the deactivation of the load buses energizing the hydraulic components, resulting in significant

water shortages even for failures originating in distant power lines. This is particularly true for power networks which are heavily loaded before the failure takes place, although severe water shortages may occur even for less critical conditions. These results showcase the strong dependency of urban water supply systems on the reliability of power networks, and suggest that approaches addressing the complexity of interconnected systems are more suitable to design resilient infrastructure. Further work may study the impact of cascading power failures on water quality or on other water networked infrastructure, such as urban drainage systems. These investigations can be respectively carried out by extending the water distribution simulation module with a water quality engine, or by replacing it with a storm-water management model [5].

5. ACKNOWLEDGMENTS

This study was partially supported by the National Research Foundation (NRF) of Singapore, under its National Cybersecurity R&D Programme (Award No. NRF2014NCR-NCR001-40).

6. REFERENCES

- [1] M. Amin. Modeling and control of complex interactive networks. *IEEE Control Systems Magazine*, 22(1):22–27, 2002.
- [2] C. D. Brummitt, R. M. D’Souza, and E. A. Leicht. Suppressing cascades of load in interdependent networks. *Proceedings of the National Academy of Sciences*, 109(12):E680–E689, 2012.
- [3] L. Buzna, K. Peters, H. Ammoser, C. Kühnert, and D. Helbing. Efficient response to cascading disaster spreading. *Physical Review E*, 75(5):056107, 2007.
- [4] H. Douglas, R. Taormina, and S. Galelli. Pressure-driven modeling of cyber-physical attacks on water distribution systems. *Journal of Water Resources Planning and Management*, doi: 10.1061/(ASCE)WR.1943-5452.0001038, 2019.
- [5] J. Gironás, L. A. Roesner, L. A. Rossman, and J. Davis. A new applications manual for the storm water management model (swmm). *Environmental Modelling & Software*, 25(6):813–814, 2010.
- [6] S. Havlin, N. A. M. Araujo, S. V. Buldyrev, C. S. Dias, R. Parshani, G. Paul, and H. E. Stanley. Catastrophic cascade of failures in interdependent networks. *Nature*, 464:1025–1028, 2010.
- [7] D. Helbing. Globally networked risks and how to respond. *Nature*, 497(7447):51, 2013.
- [8] A. Horni, K. Nagel, and K. W. Axhausen. *The multi-agent transport simulation MATSim*. Ubiquity Press London, 2016.
- [9] M. Khanabadi, H. Ghasemi, and M. Doostizadeh. Optimal transmission switching considering voltage security and n-1 contingency analysis. *IEEE Transactions on Power Systems*, 28(1):542–550, 2013.
- [10] P. Khatavkar and L. W. Mays. Model for real-time operations of water distribution systems under limited electrical power availability with consideration of water quality. *Journal of Water Resources Planning and Management*, 144(11):04018071, 2018.
- [11] Y. Koç, T. Verma, N. A. M. Arajo, and M. Warnier. Matcasc: A tool to analyse cascading line outages in power grids. *CoRR*, abs/1308.0174, 2013.
- [12] M. Korkali, J. G. Veneman, B. F. Tivnan, J. P. Bagrow, and P. D. Hines. Reducing cascading failure risk by increasing infrastructure network interdependence. *Scientific Reports*, 7, 2017.
- [13] F. Luo, C. Wang, J. Xiao, and S. Ge. Rapid evaluation method for power supply capability of urban distribution system based on n-1 contingency analysis of main-transformers. *International Journal of Electrical Power & Energy Systems*, 32(10):1063–1068, 2010.
- [14] E. Pournaras, M. Ballandies, D. Acharya, M. Thapa, and B.-E. Brandt. Prototyping self-managed interdependent networks—self-healing synergies against cascading failures. In *13th International Symposium on Software Engineering for Adaptive and Self-managing Systems (SEAMS 2018)*, 2018.
- [15] E. Pournaras, B.-E. Brandt, M. Thapa, D. Acharya, J. Espejo-Uribe, M. Ballandies, and D. Helbing. Sfina-simulation framework for intelligent network adaptations. *Simulation Modelling Practice and Theory*, 72:34–50, 2017.
- [16] E. Pournaras and J. Espejo-Uribe. Self-repairable smart grids via online coordination of smart transformers. *IEEE Transactions on Industrial Informatics*, 13(4):1783–1793, 2017.
- [17] R. Taormina, S. Galelli, H. Douglas, N. Tippenhauer, E. Salomons, and A. Ostfeld. A toolbox for assessing the impacts of cyber-physical attacks on water distribution systems. *Environmental Modelling & Software*, 112:46 – 51, 2019.
- [18] R. Taormina, S. Galelli, N. O. Tippenhauer, E. Salomons, and A. Ostfeld. Characterizing cyber-physical attacks on water distribution systems. *Journal of Water Resources Planning and Management*, 143(5):04017009, 2017.
- [19] M. Thapa, J. Espejo-Uribe, and E. Pournaras. Measuring network reliability and repairability against cascading failures. *Journal of Intelligent Information Systems*, Jul 2017.
- [20] M. Vrakopoulou, K. Margellos, J. Lygeros, and G. Andersson. Probabilistic guarantees for the n-1 security of systems with wind power generation. In *Reliability and Risk Evaluation of Wind Integrated Power Systems*, pages 59–73. Springer, 2013.
- [21] S. Wang, L. Hong, M. Ouyang, J. Zhang, and X. Chen. Vulnerability analysis of interdependent infrastructure systems under edge attack strategies. *Safety Science*, 51(1):328 – 337, 2013.
- [22] M. Zhou and S. Zhou. Internet, open-source and power system simulation. In *Power Engineering Society General Meeting, 2007. IEEE*, pages 1–5. IEEE, 2007.
- [23] R. D. Zimmerman, C. E. Murillo-Sánchez, and R. J. Thomas. Matpower: Steady-state operations, planning, and analysis tools for power systems research and education. *IEEE Transactions on power systems*, 26(1):12–19, 2011.